NAVAL POSTGRADUATE SCHOOL

MONTEREY, CALIFORNIA

THESIS

EFFECTS OF LOW-LEVEL AND DEEP-LAYER SHEAR ON SQUALL LINE INTENSITY

by

Nicolaas A. Verhoeven

June 2019

Thesis Advisor:	John M. Peters
Second Reader:	Wendell A. Nuss

Approved for public release. Distribution is unlimited.

THIS PAGE INTENTIONALLY LEFT BLANK

REPORT DOCUMENTATION PAGE			Form Approved OMB No. 0704-0188

Public reporting burden for this collection of information is estimated to average 1 hour per response, including the time for reviewing instruction, searching existing data sources, gathering and maintaining the data needed, and completing and reviewing the collection of information. Send comments regarding this burden estimate or any other aspect of this collection of information, including suggestions for reducing this burden, to Washington headquarters Services, Directorate for Information Operations and Reports, 1215 Jefferson Davis Highway, Suite 1204, Arlington, VA 22202-4302, and to the Office of Management and Budget, Paperwork Reduction Project (0704-0188) Washington, DC 20503.

1. AGENCY USE ONLY *(Leave blank)*	2. REPORT DATE June 2019	3. REPORT TYPE AND DATES COVERED Master's thesis

4. TITLE AND SUBTITLE EFFECTS OF LOW-LEVEL AND DEEP-LAYER SHEAR ON SQUALL LINE INTENSITY	5. FUNDING NUMBERS
6. AUTHOR(S) Nicolaas A. Verhoeven	
7. PERFORMING ORGANIZATION NAME(S) AND ADDRESS(ES) Naval Postgraduate School Monterey, CA 93943-5000	8. PERFORMING ORGANIZATION REPORT NUMBER
9. SPONSORING / MONITORING AGENCY NAME(S) AND ADDRESS(ES) N/A	10. SPONSORING / MONITORING AGENCY REPORT NUMBER

11. SUPPLEMENTARY NOTES The views expressed in this thesis are those of the author and do not reflect the official policy or position of the Department of Defense or the U.S. Government.

12a. DISTRIBUTION / AVAILABILITY STATEMENT Approved for public release. Distribution is unlimited.	12b. DISTRIBUTION CODE A

13. ABSTRACT (maximum 200 words)

Squall lines are a subset of mesoscale convective systems that are characterized by a long quasi-linear region of convection. Squall lines cause a wide range of weather-related impacts on society, warranting considerable research efforts to better understand their dynamics. Despite their societal impacts, there are many unknowns surrounding how vertical wind shear and entrainment affect the intensity of squall line updrafts. This paper investigated these unanswered questions using sophisticated numerical simulations from a cloud model. Low-level shear, deep-layer shear, and relative humidity are varied among a set of simulations. Increasing low-level shear, deep-layer shear, or relative humidity resulted in greater updraft velocities with larger vertical mass flux and wider updraft areas. These wide updraft areas insulate the updraft core from entrainment driven dilution and make updrafts more buoyant than in environments with weaker shear. However, these increases in buoyancy were canceled by the downward effects from the buoyancy pressure accelerations. Upward dynamic pressure accelerations increased with shear, especially at low levels, which ultimately resulted in a positive correlation between vertical accelerations, vertical velocities, and low-level and deep-layer shear. It is therefore concluded that the primary way in which shear influences squall line intensity is to enhance mechanically generated dynamic lifting along the cold pool edge and within updrafts.

14. SUBJECT TERMS squall lines, entrainment, Mesoscale Convective Systems, low-level shear, deep-layer shear	15. NUMBER OF PAGES 51
	16. PRICE CODE

17. SECURITY CLASSIFICATION OF REPORT	18. SECURITY CLASSIFICATION OF THIS PAGE	19. SECURITY CLASSIFICATION OF ABSTRACT	20. LIMITATION OF ABSTRACT
Unclassified	Unclassified	Unclassified	UU

NSN 7540-01-280-5500 Standard Form 298 (Rev. 2-89) Prescribed by ANSI Std. 239-18

THIS PAGE INTENTIONALLY LEFT BLANK

Approved for public release. Distribution is unlimited.

EFFECTS OF LOW-LEVEL AND DEEP-LAYER SHEAR ON SQUALL LINE INTENSITY

Nicolaas A. Verhoeven
Lieutenant Commander, United States Navy
BSME, Washington State University, 2006

Submitted in partial fulfillment of the
requirements for the degree of

MASTER OF SCIENCE IN METEOROLOGY AND PHYSICAL OCEANOGRAPHY

from the

NAVAL POSTGRADUATE SCHOOL
June 2019

Approved by: John M. Peters
Advisor

Wendell A. Nuss
Second Reader

Wendell A. Nuss
Chair, Department of Meteorology

THIS PAGE INTENTIONALLY LEFT BLANK

ABSTRACT

Squall lines are a subset of mesoscale convective systems that are characterized by a long quasi-linear region of convection. Squall lines cause a wide range of weather-related impacts on society, warranting considerable research efforts to better understand their dynamics. Despite their societal impacts, there are many unknowns surrounding how vertical wind shear and entrainment affect the intensity of squall line updrafts. This paper investigated these unanswered questions using sophisticated numerical simulations from a cloud model. Low-level shear, deep-layer shear, and relative humidity are varied among a set of simulations. Increasing low-level shear, deep-layer shear, or relative humidity resulted in greater updraft velocities with larger vertical mass flux and wider updraft areas. These wide updraft areas insulate the updraft core from entrainment driven dilution and make updrafts more buoyant than in environments with weaker shear. However, these increases in buoyancy were canceled by the downward effects from the buoyancy pressure accelerations. Upward dynamic pressure accelerations increased with shear, especially at low levels, which ultimately resulted in a positive correlation between vertical accelerations, vertical velocities, and low-level and deep-layer shear. It is therefore concluded that the primary way in which shear influences squall line intensity is to enhance mechanically generated dynamic lifting along the cold pool edge and within updrafts.

THIS PAGE INTENTIONALLY LEFT BLANK

TABLE OF CONTENTS

THIS PAGE INTENTIONALLY LEFT BLANK

LIST OF FIGURES

THIS PAGE INTENTIONALLY LEFT BLANK

LIST OF TABLES

THIS PAGE INTENTIONALLY LEFT BLANK

LIST OF ACRONYMS AND ABBREVIATIONS

3D	three-dimensional
BPA	buoyancy pressure accelerations
CM1	Cloud Model 1
DL	deep-layer
DPA	dynamic pressure accelerations
LL	low-level
OFB	outflow boundary
RH	relative humidity

THIS PAGE INTENTIONALLY LEFT BLANK

I. INTRODUCTION

Throughout history, thunderstorms have always been a natural occurrence of terrifying beauty. With the help of science, humans have evolved from believing thunderstorms were controlled by the gods to studying the convection associated with their generation and intensification. As technology advanced, the way we studied convective storms also advanced. In the 1940s, R. A. Hamilton and J. W. Archbold (1945) used physical observations recorded across Nigeria and West Africa to enhance forecasting in that geographic area. Thirty years later, experimental data gathered from a squall line that passed over sensors networks during the Global Atmospheric Research Programme's Atlantic Tropical Experiment (GATE), expanded the understanding of the structure, dynamics, and life cycle of the system (Houze 1977). Today, high-powered computer modeling is being used to supplement experimental data and was recently employed to investigate the effects of cold pools on the intensity of convective systems (Lebo and Morrison 2015).

A Mesoscale Convective System (MCS) is an organized grouping of thunderstorms with a range scale of 100 kilometers (American Meteorological Society 2019). MCSs are responsible for a large percentage of the societal impacts posed by thunderstorms, including torrential rain and flooding (Schumacher and Johnson 2005), damaging straight-line wind (e.g., Johns and Hirt 1987; Johns and Doswell 1992; Guastini and Bosart 2016), excessive lightning (e.g., Rutledge and MacGorman 1988; Holle et al. 1994; Markowski et al. 2013), and tornadoes (e.g., Gallus et al. 2008). Squall lines are a subset of MCSs that are characterized by a nearly continuous line of updrafts. Squall lines usually form along the boundary of a cold front, within the warm sector of a developing cyclone, or along a warm front (e.g., Parker and Johnson 2000). They can also form along the edges of merged cold pools in the absence of large-scale synoptic features, and frequently occur in the tropics as well as the mid-latitudes. They can last anywhere from minutes to hours. Gusty (sometimes damaging) winds, large seas, frequent lightning, and heavy rainfall and hail are all frequently associated with squall lines.

Squall lines occur over both oceans and land with regular frequency. The United States averages 100,000 thunderstorms every year with roughly 10% being severe. The storms are classified as being severe if they have wind gusts over 50 knots or hail greater than 1 inch (National Severe Storms Laboratory 2019).

Most of the damage from squall lines comes from high winds or torrential rains. But damage from heavy rain can depend on the land area affected by the squall line. Land areas with great drainage and water retention are not as affected by significant rain fall as flatter areas, already saturated with water. Whereas, damage from high winds is more or less land area nonspecific. For example, bow echoes are bow shaped radar returns that form on the leading edge of a squall line and are associated with damaging straight-line winds (e.g., Johns 1993). The maximum winds of a bow echo are located at the leading edge of the bow shape. Figure 1 shows the radar return of a mature squall line in Fort Wayne, IN, with two bow echoes along its eastern front.

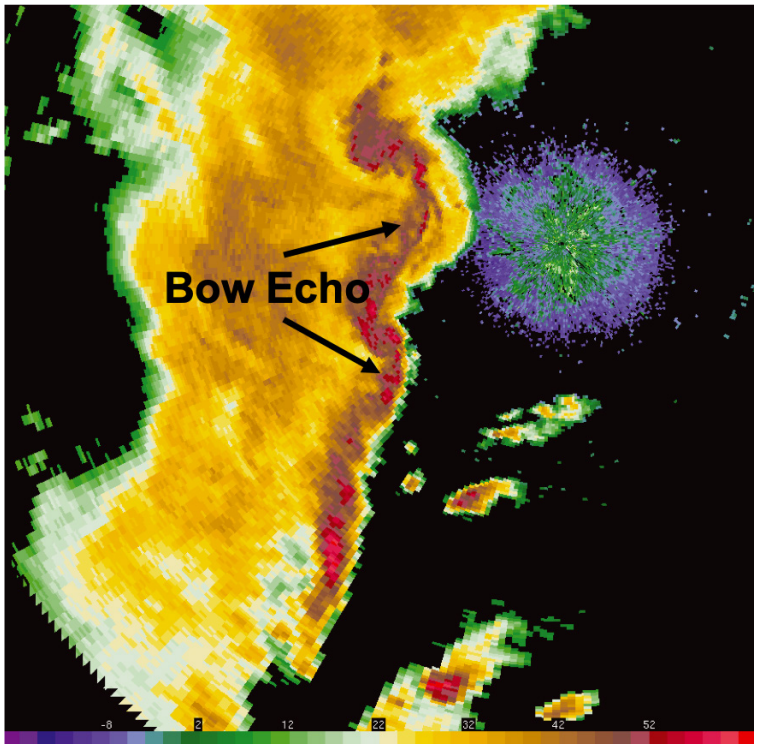

Figure 1. Radar return of a bow echo.
Source: Markowski and Richardson (2010).

An example of a deadly and damaging squall line occurred in July of 2018. In this event, a duck boat on the Table Rock Lake near Branson, MO, sank during the passage of an intense squall line, killing 17 people. A thunderstorm watch was issued for the area and was followed, six hours later, by several evolving severe thunderstorm warnings. The area forecast warned that wind gusts up to 70mph with a storm speed of 65mph were expected over the lake. It is estimated that that the duck boat capsized in high winds and waves less than 30 minutes after receiving the severe thunderstorm warning (Erdman 2018). The duck boat case study is one example of how destructive squall lines can be.

The Navy must be able to operate under any conditions in order to maintain its global reach. As frequently and severe as squall lines occur, they have a direct impact on the operations of Navy ships and aircraft. Understanding of how squall lines intensify or weaken can lead to better forecasting and help Navy assets manage the risks associated with severe weather.

THIS PAGE INTENTIONALLY LEFT BLANK

II. BACKGROUND

Squall lines typically form when the rain cooled outflow of individual storms merge into a cold pool that is much larger than the individual storm cells. Convection often organizes into a line along the edge of the cold pool called the "outflow boundary," or OFB. This convection is organized by the locally enhanced lifting along the edge of the cold pool, which facilitates the continuous regeneration of new convective cells (Rotunno et al. 1988) in which new squall line elements formed ahead of the older mature elements (Houze 1977). Houze (1977) determined that the highest and most destructive winds are generated at the OFB, beneath the most intense convection. Because of the large societal impacts of squall lines, considerable research efforts are warranted to determine what environmental characteristics determine squall line intensity.

Shear is a dominate factor that influences the evolution of squall lines (e.g., Rotunno et al. 1988; Weisman and Rotunno 2004; Coniglio et al. 2006). Previous studies have often separately investigated the influence of low-level shear (e.g., shear in the lowest few kilometers of the atmosphere) and deep-layer shear (e.g., shear through a depth of 6 or 8 kilometers) on squall line intensity. When strong low-level shear interacts with the edge of a cold pool an upward dynamic pressure gradient force is created, lifting air parcels to the level of free convection. The resultant strong mechanically forced lifting readily generates new convective cells along the edge of the cold pool. The low-level shear interacting with cold pools is thought to be essential to sustaining long-lived squall lines (Rotunno et al. 1988; Weisman and Rotunno 2004). The strength of squall lines also positively correlates with the magnitude of deep-layer shear (Coniglio et al. 2006); however, the dynamics responsible for this connection are less understood than that of low-level shear. Furthermore, the relative importance of low-level and deep-layer shear in squall line intensity has been debated over the past few decades. Rotunno et al. (1988) and Weisman and Rotunno (2004, 2005) argue that low-level shear is a dominant factor with deep-layer shear being of secondary importance, whereas Stensrud et al. (2005) and Coniglio et al. (2006) argue for the importance of both low-level and deep-layer shear in squall line intensity. While there is some compelling evidence for either side of this

argument, there remains unanswered questions about the interactions between both low-level and deep-layer shear and squall lines. For instance, previous studies have only analyzed the influence of shear on vertical accelerations within the lowest few kilometers of the atmosphere (e.g., Bryan and Rotunno 2014), which is below the majority of convective updrafts (refer to the previous discussion on vertical pressure gradient accelerations along the cold pool edge). It is unclear what the direct effect of low-level and deep-layer shear have on vertical accelerations within updrafts, and as a consequence the dynamical linkage between shear and updraft intensity remains somewhat obscure.

One dynamical connection between deep-layer shear and squall line intensity that has not been thoroughly explored is entrainment. Entrainment is the mixing of environmental air into the MCS. The air can vary in moisture content and/or temperature which has different effects on the intensification of the squall line. Zipser and Ferrier (2000) studied the effects of entrainment and shear on the low and mid-levels of the troposphere. They found that squall lines intensified and produced more precipitation in situations where entrained air was moist, relative to situations where the entrained air was comparatively dry. However, due to the limitations on computing power at the time, their models were run in 2D and their results would benefit from a higher resolution 3D model run.

Previous authors have speculated that shear should influence entrainment in convection by making the updraft buoyancy more dilute than it would be if no shear were present (e.g., Markowski and Richardson 2010), though Peters et al. (2019) showed that the influence of shear-driven dilution is minimal for growing cumulus congestus clouds. In fact, Peters et al. (2019) showed that strong vertical shear creates more low-level inflow, wider updrafts, and less dilute or more buoyant updrafts in supercells than that of ordinary convection. This shows that vertical wind shear actually decreased the effects of entrainment on convection and facilitated more buoyant updrafts in environments with strong deep-layer shear compared to environments with weak deep-layer shear. Unfortunately, few previous studies have comprehensively quantified this effect in the context of squall lines, which are dynamically distinct from cumulus congestus and supercells.

The goal of this paper is to uncover dynamical linkages between shear, entrainment, and vertical accelerations within 3D models. Since the deleterious effects of entrainment on buoyancy and the characteristics of vertical pressure gradient accelerations are both essential elements that determine a storms' intensity, a thorough investigation of these quantities is warranted. The primary research questions that are investigated in this paper are: What are the influences of shear on vertical pressure gradient accelerations in squall lines? How is entrainment influenced by vertical wind shear, and what are the subsequent impacts of shear-driven changes to entrainment on squall line on buoyant accelerations in squall lines? The following hypotheses are addressed:

1. Both low-level and deep-layer shear conspire to reduce the rate at which updraft cores are diluted via entrainment. Consequently, squall lines in stronger shear are stronger than those in weaker shear because the former have larger updraft buoyancies.

2. Both low-level and deep-layer shear positively correlate with the magnitude of upward dynamic accelerations in squall lines, making vertical velocities larger when squall lines are experiencing larger vertical shear.

This thesis will describe the methods used to test the hypotheses, analyze and discuss the results and finally, recommend areas for future research. The organization is as follows: Chapter III describes the setup for numerical modeling experiments and the methods that were used to analyze data from numerical models; Chapter IV discusses the results from data analysis; finally, Chapter V summarizes the results, lists conclusions, relates this work to other research, and outlines avenues for future investigation.

THIS PAGE INTENTIONALLY LEFT BLANK

III. METHODS

To investigate the hypotheses presented in this paper, a realistic atmospheric model will be utilized. Cloud Model 1 (CM1) was the ideal atmospheric model, selected because it is freely available, tailored for modeling deep convection, and is widely used in the academic community. CM1 is a nonhydrostatic three-dimensional numerical model, engineered specifically for high-resolution modeling, and developed at Pennsylvania State University and the National Center for Atmospheric Research (Bryan and Fritsch 2002).

All CM1 model runs were initialized with the same thermodynamic sounding (Figure 2), which is known to cause deep convection. The sounding was first used by Rotunno et al. (1988) and represents a typical thermodynamic sounding of a midlatitude squall line and has been used in academic research for decades. The boundary layer moisture in this profile was set to 14 g kg^{-1}, yielding a 0-1 kilometer mean convective available potential energy of ~ 1730 J kg^{-1}. The sounding's mid-troposphere relative humidity was modified for the specific experiments in this thesis, and these modifications will be discussed in more detail later in this paper.

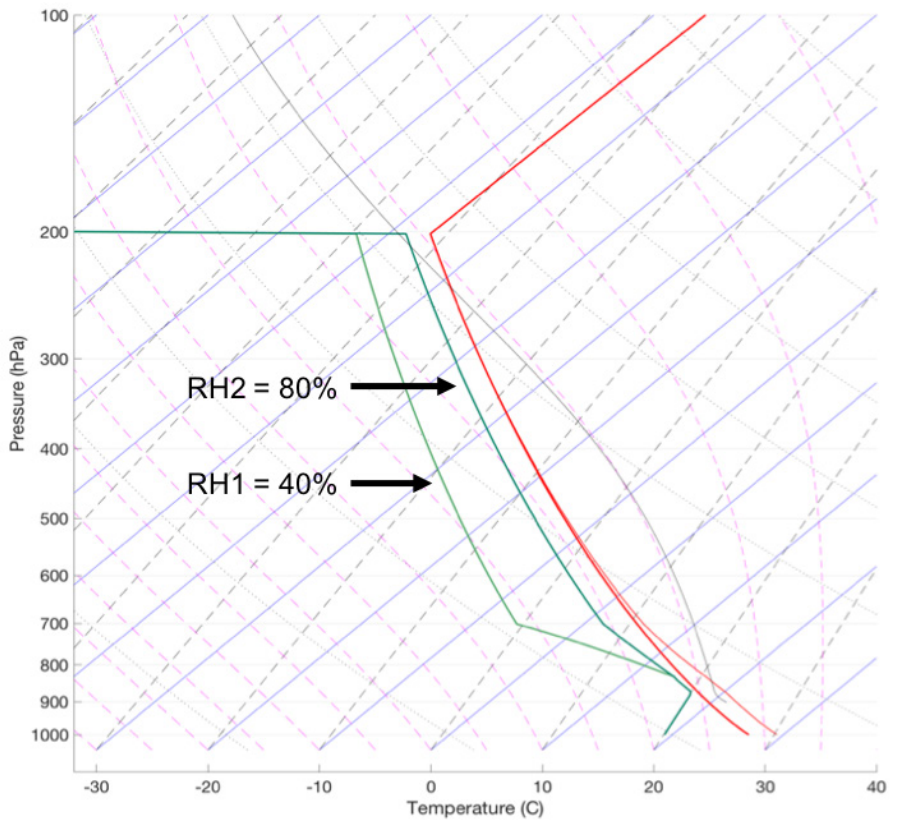

A skew-T diagram of the initial sounding used for all model runs. The light green line on the left is used for model runs with the relative humidity of 40% and the dark green line on the right if used for model runs with the relative humidity of 80%. The grey line represents the temperature for a lifted air parcel with the average properties of the lowest 1 kilometer of the atmosphere.

Figure 2. Cloud Model 1 initial sounding

The model was run in a three-dimensional box with dimensions of 250 kilometers in the x direction and 100 kilometers in the y direction. The grid spacing was set at 2 kilometers in both Δx and Δy direction. The height in the z direction was set to 18 kilometers and the grid spacing varied horizontally to have the finest resolution in the areas of greatest concern. The grid spacing was 100 meters from 0 kilometers to 2 kilometers, then increased linearly from 2 kilometers to 7 kilometers, and finally, 250 meters for heights greater than 7 kilometers. The model simulated a 6-hour period with a sampling frequency of every 5 minutes. Lateral boundary conditions were periodic in the north and south directions, and open radiative in the east and west directions.

To develop a squall line, a cold pool was inserted from the ground up to a height of 1.5 kilometers and from the boundary at 0 kilometers to the center of the box at 125 kilometers in the x direction, and from 0 kilometers to 100 kilometers in the y direction. The temperature deficit of the cold pool was -7 kelvin at the surface, and decreased linearly to 0 kelvin at 1.5 kilometers. A passive tracer was inserted with a maximum concentration value of 1 outside the cold pool and below 1.5 kilometers, and 0 elsewhere (Figure 3). Passive tracers act as a conserved quantity in CM1, with the only source and sink term following an air parcel being the model's sub-grid scale mixing scheme. This passive tracer was used to assess the degree to which updrafts in the squall line were diluted via entrainment. Updrafts that are less diluted will have larger tracer concentrations, indicating a higher percentage of air having originated from the high CAPE boundary layer. Conversely, updrafts that are more diluted will have lower tracer concentrations, indicating a larger percentage of their mass originated from the inward penetration of mid-level environmental air. Finally, to facilitate the development of a realistically heterogeneous 3-D squall line structure, random temperature perturbations were added to the initial conditions below the level of the top of the cold pool. These random perturbations were evenly distributed with a maximum amplitude of 1 K.

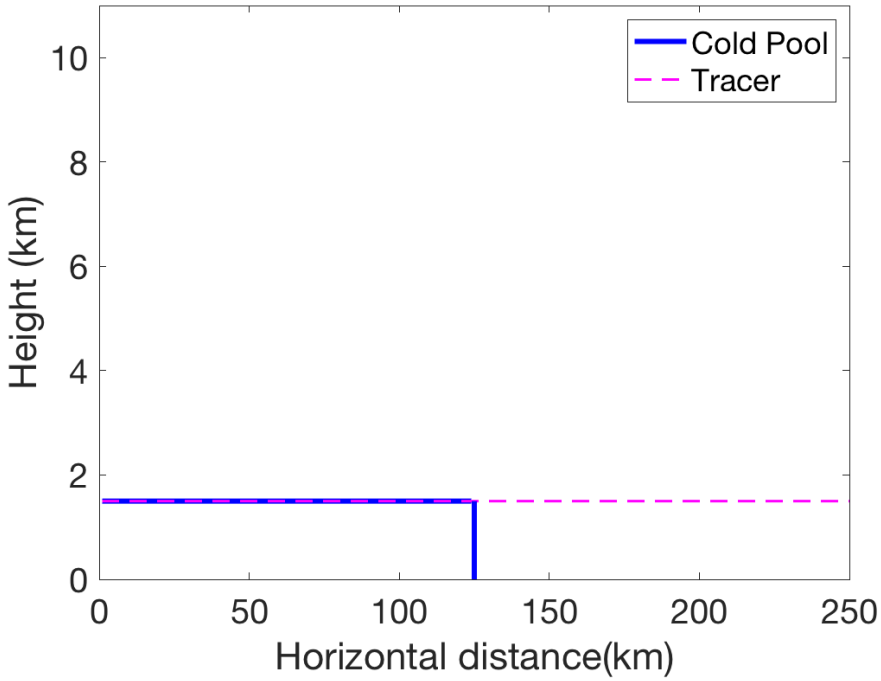

Figure 3. Initial conditions of the cold pool and passive tracer

In order to test the hypothesis relating to wind shear, analysis was conducted by varying the u component wind to create different low-level (LL) wind shear and deep-layer (DL) wind shear values. The relative humidity (RH) was varied above 3 kilometers for each model run to test its effects on entrainment as well (the RH above the tropopause was set to 0 for simplicity). For connections between shear and squall line intensity that are strongly dependent on entrainment, we expect larger differences in squall line behavior as a function of environmental shear when RH is lower. This is because the deleterious evaporative effects of the entrainment of environmental air are more pronounced for dry ambient environments than for moist ambient environments.

A total of 18 model runs (Table 1) were conducted using 3 different values for each shear parameter and two different RH values. The RH middle-tropospheric values were set at 40% and 80% and held constant throughout the entire 6-hour model run. To modulate low-level shear among runs, the u component wind varied linearly from minimum values of -6 m s^{-1}, -11 m s^{-1}, and -17 m s^{-1}at the surface to 0 m s^{-1}at the top of the cold pool (Figure 4). To modulate deep-layer shear among runs, the u component wind varied linearly from

0 m s^{-1} at the height of the top of the cold pool to 0 m s^{-1}, 7 m s^{-1}, and 12.5 m s^{-1} at 10 kilometers (Figure 4). These shear magnitudes were more-or-less arbitrarily determined, but are consistent with the observed shear magnitudes in MCS environments (e.g., Coniglio et al. 2010, Figures 12 and 13). The purpose for examining both variations in low-level shear and deep-layer shear is because (1) previous authors have not investigated linkages between low-level shear and entrainment, and (2) the potential feedbacks between low-level and deep-layer shear are largely unexplored. This paper intends to address these unanswered questions.

Table 1. Naming convention for each of the 18 CM1 model runs

Relative Humidity 40% (RH1)

Low-Level Shear Values (m s^{-1})	Deep-Layer Shear Values (m s^{-1})		
	0	7	12.5
-6	**LL1_DL1_RH1**	**LL1_DL2_RH1**	**LL1_DL3_RH1**
-11	**LL2_DL1_RH1**	**LL2_DL2_RH1**	**LL2_DL3_RH1**
-17	**LL3_DL1_RH1**	**LL3_DL2_RH1**	**LL3_DL3_RH1**

Relative Humidity 80% (RH2)

Low-Level Shear Values (m s^{-1})	Deep-Layer Shear Values (m s^{-1})		
	0	7	12.5
-6	**LL1_DL1_RH2**	**LL1_DL2_RH2**	**LL1_DL3_RH2**
-11	**LL2_DL1_RH2**	**LL2_DL2_RH2**	**LL2_DL3_RH2**
-17	**LL3_DL1_RH2**	**LL3_DL2_RH2**	**LL3_DL3_RH2**

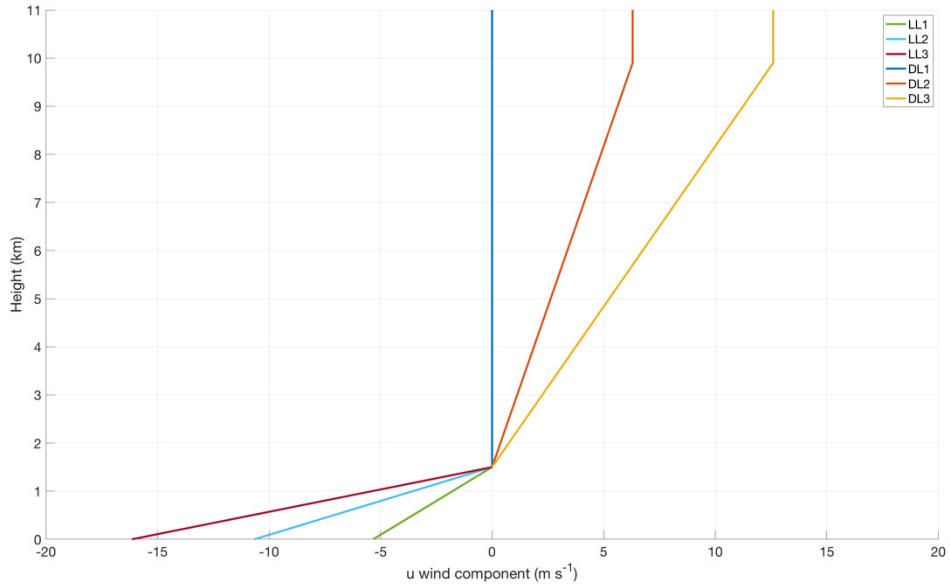

Figure 4. Variation of u component wind for each model run

Each of the 18 model runs were analyzed to determine if the initial conditions caused the squall line to intensify and mature or to weaken and die. Three metrics were used in evaluating squall line intensity. The first was the total vertical mass flux, which is a measurement of the total amount of air going up in the squall line. Total vertical mass flux was calculated by

$$M \equiv \iint \rho w_{up} d\sigma \tag{1}$$

where M is the vertical mass flux, ρ is air density, w_{up} is the vertical velocity of the updrafts, and σ is the cross-sectional area of all of the updrafts. The larger the vertical mass flux, the more vigorous the convective overturning. Peters et al. (2019) showed that increasing deep-layer shear resulted in stronger low-level inflow and stronger subsequent vertical mass flux in updrafts. This increase in vertical mass flux made updrafts wider and more shielded from entrainment. Vertical mass flux is therefore an ideal starting point for uncovering connections between shear and entrainment. The second metric analyzed was the maximum grid point vertical velocity within the domain. The larger the maximum vertical velocity, the more intense the updraft. The last metric was maximum surface wind speed. The larger the maximum surface wind speed, the greater potential for near-surface

wind damage. This metric will help determine if the shear influences on updraft intensities has any bearing on the potential for damaging near-surface winds.

In order to physically connect environmental shear to updraft intensities, three physical factors were considered. The first was the maximum updraft buoyancy at each level within the model domain. The more buoyant updrafts indicate less dilution from entrainment. Larger buoyancy equates to stronger vertical accelerations and stronger updraft velocities. The second factor was maximum updraft tracer concentration. As discussed earlier, a lower updraft tracer concentration means the updraft has been diluted by entrainment. The third factor analyzed was vertical perturbation pressure gradient force, which is

$$PGF = -\frac{1}{\rho}\frac{\partial p'}{\partial z} \tag{2}$$

The larger the vertical pressure gradient force, the stronger the vertical accelerations and updraft velocities. Vertical accelerations are commonly divided into dynamic and buoyant components, so that the vertical momentum equation may be written as

$$\frac{Dw}{Dt} = B \quad \underbrace{-\frac{1}{\rho_0}\frac{\partial p'_b}{\partial z}}_{\substack{Buoyancy\\ Pressure\\ Acceleration\ (BPA)}} \quad \underbrace{-\frac{1}{\rho_0}\frac{\partial p'_d}{\partial z}}_{\substack{Dynamic\\ Pressure\\ Acceleration\ (DPA)}} \tag{3}$$

$$with \quad B = g\left[\frac{\rho'}{\rho_0} - \frac{\rho_i}{\rho_0}\right]$$

where ρ_0 is the initial density, ρ' is the perturbation dry air density, and ρ_i is the density of the ith hydrometric reading (rain, snow, etc). The buoyant and dynamic components of pressure are given by the following equations:

$$\nabla^2 p'_b = \frac{\partial \rho_0 B}{\partial z} \tag{4}$$

$$\nabla^2 p'_d = \nabla \cdot [\rho_0 (\boldsymbol{V} \cdot \nabla)\boldsymbol{V}] \tag{5}$$

These pressure components were computed from model output by first calculating the right-hand side of the equations using centered 2nd order finite difference approximations to derivatives. A two-dimensional fast Fourier transform was then applied to the data to

reduce the elliptic equations to a tri-diagonal system of linear equations. This tri-diagonal system was then solved using a tri-diagonal algorithm. The resulting solved equation system was then inverse Fourier transformed to obtain the buoyant and dynamic pressure contributions. This method is identical to the CM1 source code that solves for the pressure field when the model is run in anelastic mode.

Dynamic pressure accelerations (DPA) are primarily driven by spatial gradients in wind velocity. In squall lines, these accelerations occur in areas of horizontal convergence, along the edge of outflow boundaries; which creates local high pressure and upward dynamic pressure accelerations (Bryan and Rotunno 2014). The stronger the low-level shear, the stronger the convergence along outflow boundaries and the stronger upward dynamic pressure accelerations. Similar convergence between shear over deeper layers and flow within updrafts may potentially result in deep-layer shear enhancing dynamic accelerations throughout the depth of updrafts.

Buoyancy pressure accelerations (BPA) result from the presence of localized gradients in buoyancy. For instance, the presence of cold air within cold pools relative to the adjacent comparatively warm environment results in upward BPA along outflow boundaries. Likewise, the presence of vertical gradients in buoyancy below and above updrafts results in low pressure at updraft base, high pressure at updraft top, and a downward oriented BPA within the updraft (e.g., Morrison 2016, Peters 2016). A potential linkage between shear and buoyant pressure accelerations is the tendency for shear to make slanted updrafts, and the dependency of BPA on updraft slant (e.g., Parker 2010). Another potential linkage is that wider updrafts tend to have larger downward oriented BPA than narrow updrafts (e.g., Morrison 2016, Peters 2016).

IV. RESULTS

For an initial qualitative understanding of how shear effects the intensity of squall lines, an average vertical cross-section composite was generated. Each composite visually shows the cloud and ice water mixing ratio, θ'contours, vertical velocity contours, and wind vectors. Each figure contains both relative humidity values and is arranged by low-level shear values with Figure 5 comprised of LL1, Figure 6 comprised of LL2, and Figure 7 comprised of LL3. The size of the updraft was assessed by comparing the area overlapping the vertical velocity (red contours) with the cloud and ice water mixing ratio in the composites (colored area). These figures demonstrate that convective area increases as a response to increasing low-level and deep-layer shear, and increasing RH, with the largest updraft areas occurring at in the LL3_DL3_RH2 model run. By holding the low-level shear value constant, trends in the deep-layer shear become more apparent. Increasing the deep-layer shear makes the updraft less slanted and more upright, based upon the appearance of the cross-section parallel wind vector arrows in the updraft region. This is most prominent in Figure 7, as the updraft grows with increasing deep-layer shear it becomes wider and more vertical. Squall line intensity can be estimated by looking at the area of highest convection (multiple red contours overlapping the darkest shading). As shear and RH increase, squall line intensity increases, with the most intense squall line occurring during the LL3_DL3_RH2 model run.

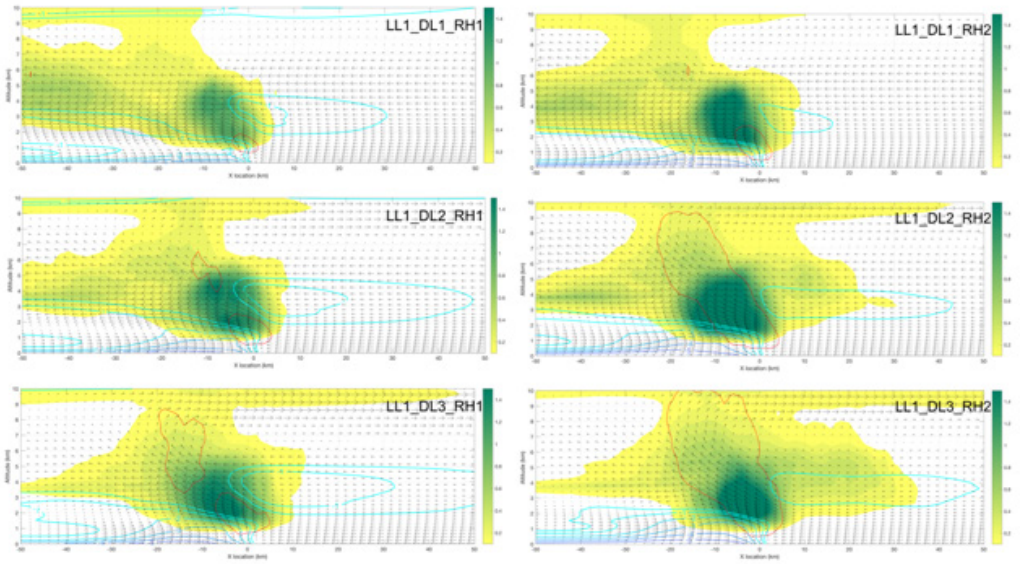

The shaded area is of the cloud and ice water mixing ratio in g kg^{-1}. Blue contour is of θ' in decreasing increments of -1K. The red contour is of vertical velocity in increments of 3 m s^{-1}. The arrows are streamline magnitudes of wind speed in m s^{-1}.

Figure 5. Vertical squall line composite of all LL1 shear values for RH1 and RH2

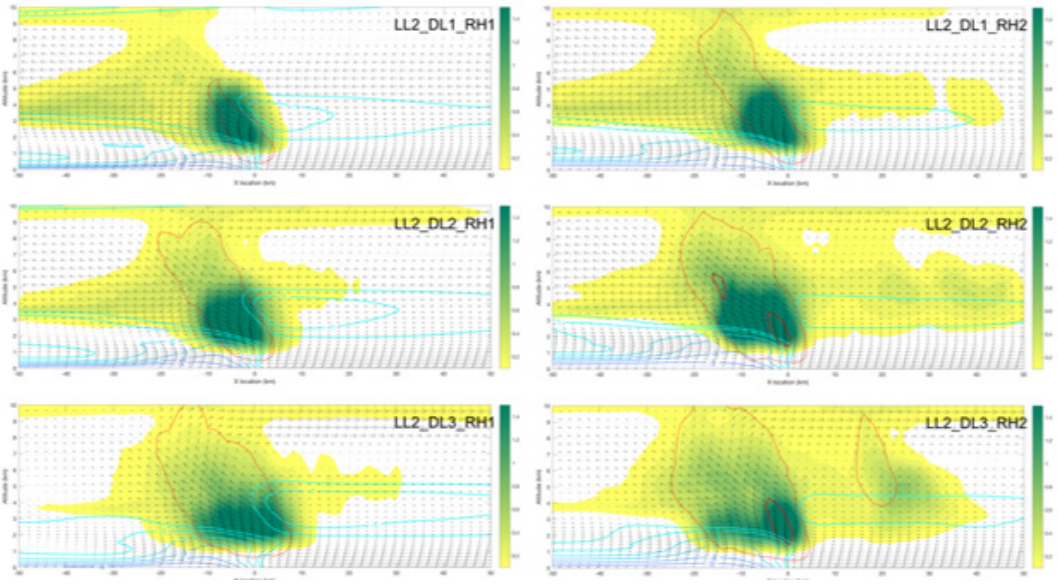

The shaded area is of the cloud and ice water mixing ratio in g kg^{-1}. Blue contour is of θ' in decreasing increments of -1K. The red contour is of vertical velocity in increments of 3 m s^{-1}. The arrows are streamline magnitudes of wind speed in m s^{-1}.

Figure 6. Vertical squall line composite of all LL2 shear values for RH1 and RH2

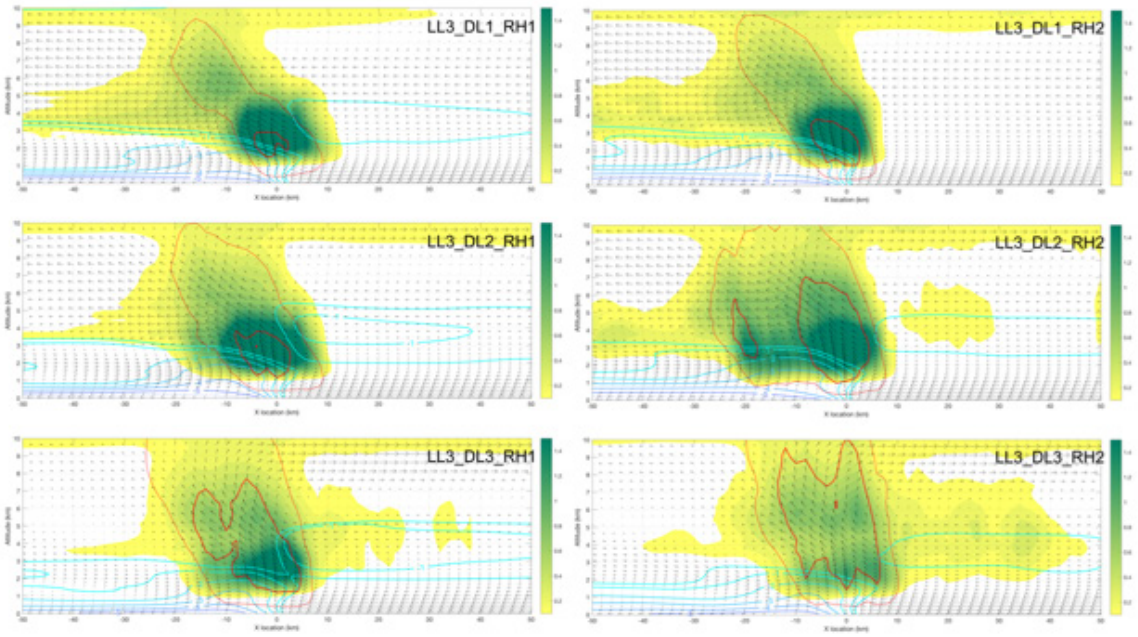

The shaded area is of the cloud and ice water mixing ratio in g kg^{-1}. Blue contour is of θ' in decreasing increments of -1K. The red contour is of vertical velocity in increments of 3 m s^{-1}. The arrows are streamline magnitudes of wind speed in m s^{-1}.

Figure 7. Vertical squall line composite of all LL3 shear values for RH1 and RH2

Next, a quantitative assessment of the differences in squall line intensity was conducted. In order to determine how shear effects squall line intensity, two related line-plots were created. They were grouped into two relative humidity plots, with a common base color is used for each RH value. Cooler colors were associated with RH1 and warmer colors are associated with RH2. Each plot has 3 low-level (LL) shear values and 3 deep-layer (DL) shear values for a total of 9 unique wind profiles. Low-level shear values are differentiated by line color. As low-level shear values increase, the lines become darker shades of the base color. Equivalent low-level shear values will have the same line color. Deep-layer shear values are differentiated by dotted, dashed, and solid lines. As deep-layer shear values increase, the line becomes more solid and bolder. Equivalent deep-layer shear values will have the same line thickness and style. Table 1 shows each RH group, model run naming convention, and associated values. It will be a useful reference when analyzing the remaining figures.

To examine differences in long-term trends among the simulations, rather than instantaneous fluctuations, each plot was averaged over the last 3 hours of the 6-hour model run, when the squall line was mature. The only exception was the plot of maximum vertical velocity which displays a time series plot of the final 3 hours of the squall line. To highlight data trends and make evaluations easier, one model run was selected as the baseline and subtracted from the other model runs to create difference plots. LL1_DL1_RH1 was selected as the baseline because it has the lowest low-level shear, deep-layer shear, and relative humidity values. Additionally, the data analyzed only comes from areas with significant updrafts. In order to isolate the updrafts from downdrafts and non-convective regions, updrafts were defined as grid points that corresponded to vertical velocities that exceeded 3 m s^{-1} and the sum of the cloud and ice water mixing ratio exceeded 10^{-2} g kg^{-1}.

The effects of shear on vertical updraft intensity was analyzed using a time series of maximum vertical velocity. The maximum vertical velocity plots are shown in Figure 8. Maximum vertical velocities were generally larger for both larger magnitudes of low-level and deep layer shear, than for smaller shear magnitudes. This indicates that, generally, both low-level and deep-layer shear make squall line updrafts more intense. Maximum vertical velocity was more responsive to the deep-layer wind shear magnitude, having increased ~ 5 m/s for each incremental increase in deep-layer shear (dotted line progresses to solid). Responses to low-level shear (light color progresses to black) were less pronounced with ~ 1-2 m/s increases in maximum vertical velocity for incremental increases in low-level shear.

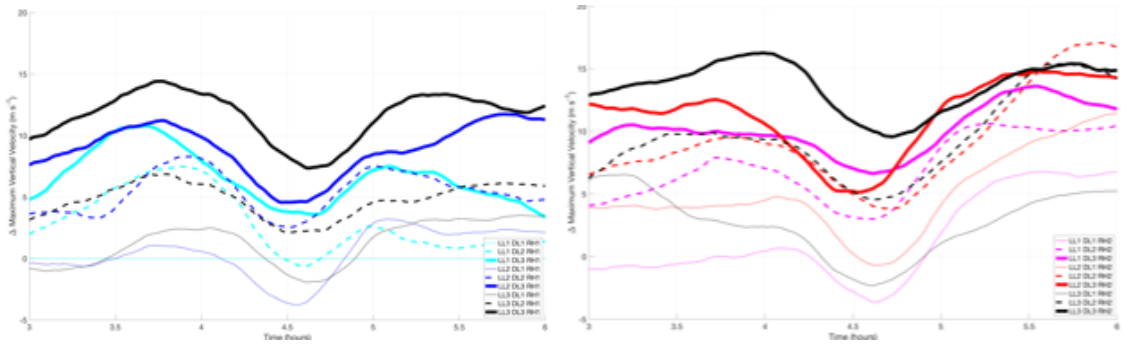

Figure 8. Time series of maximum vertical velocity within all updrafts

In order to uncover the physical mechanisms behind the differences in updraft vertical velocities among simulations, the vertical distributions of the individual acceleration terms in Equation (3) are examined. The differences in the vertical distribution of average buoyancy through the updrafts was analyzed first. Looking at Figure 9, buoyancy generally becomes more negative below 3 km with both increasing low-level (color darkens) and increasing deep-layer (line thickens) shear magnitudes. This is likely a result of progressively larger amounts of negatively buoyant cold pool air being ingested by updrafts as the squall line became more intense. Grant et al. (2018) has a detailed discussion of this process. This increase in negative buoyancy with increasing shear was more pronounced for incremental increases in low-level shear. Above 3 km however, both increasing low-level and deep-layer shear make updrafts appreciably more buoyant, which supports the second hypothesis that shear affects squall line intensity by protecting the interiors of their updrafts from entrainment-driven dilution. The relationship between buoyancy and entrainment is supported by the fact that the range of buoyancy values above 3 km, as a function of low-level and deep-layer shear, was larger in the low RH runs than in the high RH runs. The values vary more because the lower RH runs (ΔB ranged from 0 to 0.07 m s^{-2} at 10 km in the RH1 runs, whereas ΔB only ranged from 0.65 to 0.15 m s^{-2} at 10 km in the RH2 runs). would have been more sensitive to evaporation as dry air was entrained. The higher RH runs experience less entrainment and have less variation in their buoyancy values.

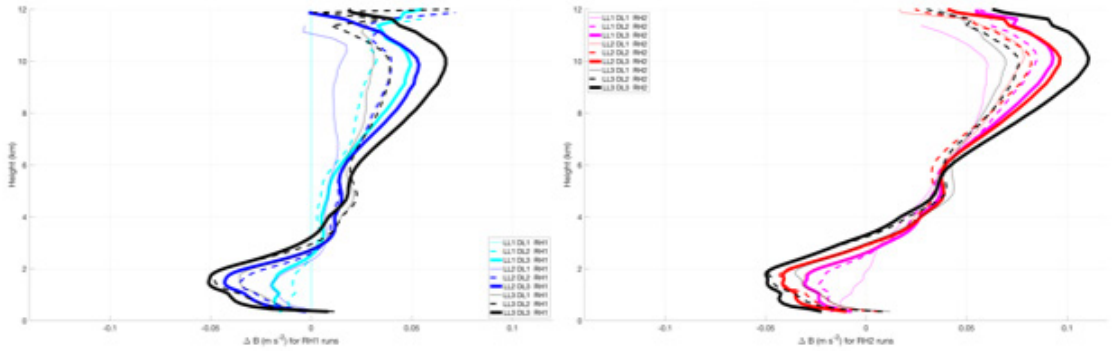

Figure 9. Differences in the horizontal average of updraft buoyancy (ΔB) between a given simulation, and the LL1_DL1_RH1 simulation

In order to understand more about the effects of shear on entrainment, the updraft maximum tracer concentration was analyzed. Higher tracer concentrations equate to less entrainment-driven dilution of updraft cores. Plots of the average tracer concentration are shown in Figure 10. Generally, increasing both low-level (color darkens) and deep layer (line thickens) shear increases the average updraft tracer concentration, further supporting the second hypothesis that shear makes updrafts less susceptible to entrainment-driven dilution. However, there are some complexities to this relationship. For instance, the relationship between low-level shear and tracer concentration is much less pronounced for the runs with the weakest deep-layer shear, which is probably a result of complicated nonlinear interactions between entrainment and other updraft processes.

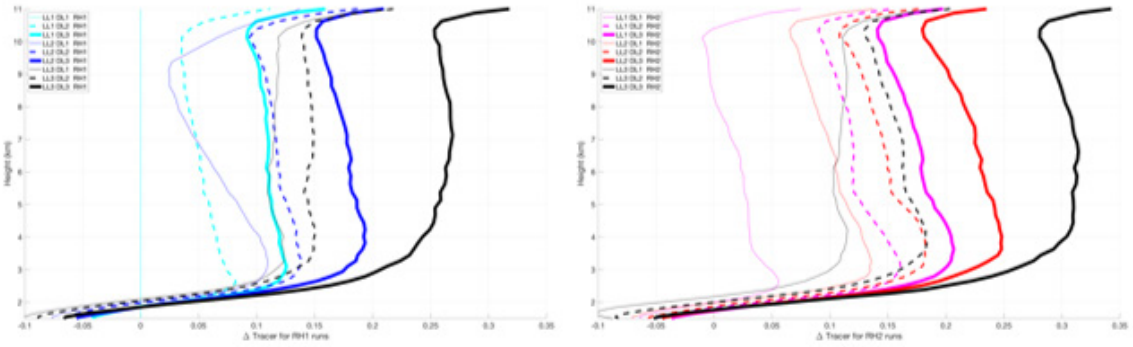

Figure 10. As in Figure 6, but for updraft averaged tracer concentration

The data presented so far suggests that vertical wind shear does indeed influence squall line intensity through its relationship with entrainment. Higher shear generally equates to lower entrainment driven dilution of updrafts. So why does shear makes updrafts less dilute? Hypothesis two states that updrafts were wider as a result of the shear, which was responsible for the decreased susceptibility to entrainment driven dilution. To examine this idea, the effects of shear on average vertical mass flux was analyzed. Vertical mass flux is a function of updraft vertical velocity and updraft area. Higher vertical mass flux values therefore indicate either stronger vertical velocities, and/or wider updrafts. The average vertical mass flux is shown in Figure 11. Much like the previous cases, increasing either low-level (color darkens) or deep-layer (line thickens) shear increased vertical mass flux, with RH2 having higher vertical mass flux values.

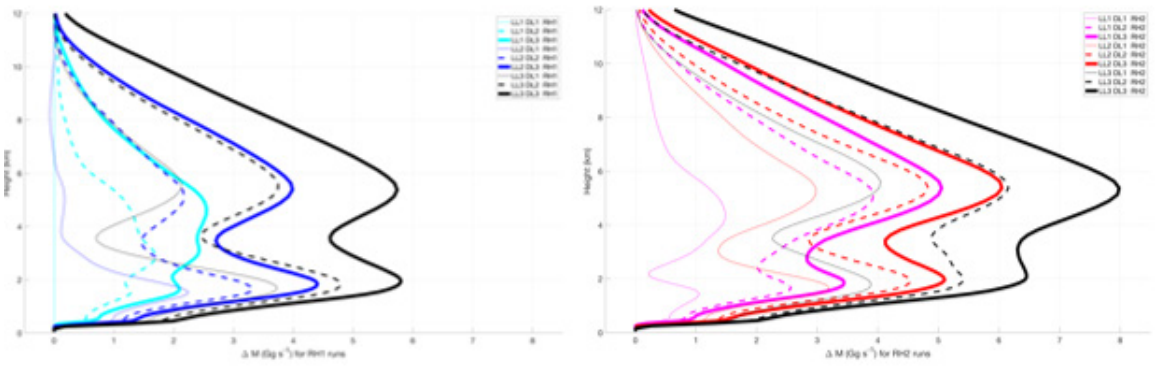

Figure 11. As in Figure 6, but for total vertical mass flux

Since vertical mass flux is proportional to both vertical velocity and updraft area, the differences in updraft area must be examined to determine whether updrafts were indeed wider in more strongly sheared environments. Figure 12 shows the average total updraft area. Indeed, it is evident that the vertical distribution of differences in updraft area is closely tied with vertical mass flux, showing that updraft area becomes larger when more shear is present.

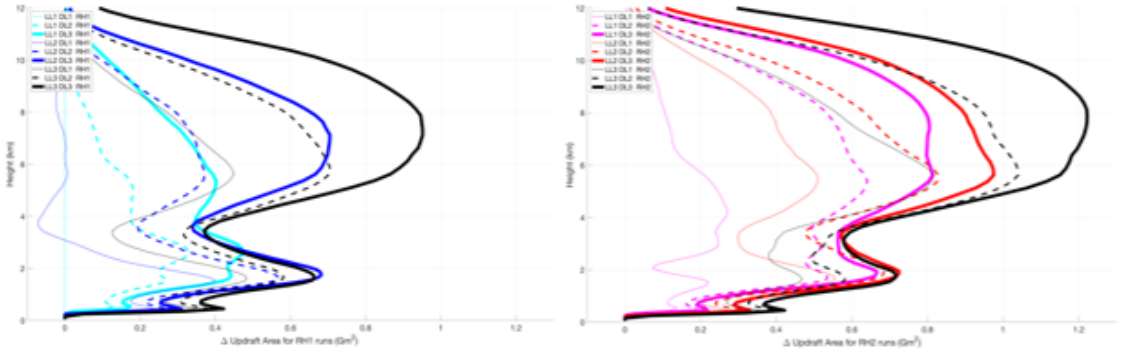

Figure 12. As in Figure 6, but for total updraft area

The previous paragraphs demonstrate clear support for hypothesis one; however, as was discussed in section III, changes to buoyancy, updraft area, and updraft slant also have influences on BPA. Based upon Figures 4-7, updrafts appear to become less slanted as shear increases. This suggests that downward BPA might decrease with increasing shear; however, updrafts becomes considerably wider with increasing shear, suggesting that downward BPA might increase with increasing shear. Figure 13 shows the effects of shear on average BPA. In the lowest levels of the atmosphere, increases in shear caused BPA to increase. The opposite was true in the deep levels, where increased shear caused BPA to decrease. Comparing the shape of the average vertical buoyancy plots (Figure 9) with the BPA plots, it is clear that they are negatively correlated. These findings are consistent with past theoretical and modeling studies (e.g. Morrison 2016 a, b; Peters 2016). It is often useful to examine the sum of buoyancy and BPA, known as effective buoyancy pressure acceleration (EBPA) and shown in Figure 14, to determine the overall influence of the updraft's thermodynamic fields on vertical accelerations. Interestingly, the results show that progressively larger shear values actually make EBPA progressively smaller. This is likely because, wider updrafts tend to have larger downward BPA than narrower updrafts, all else being equal (e.g. Morrison 2016). Therefore, any gains in upward buoyant acceleration from increasing shear values are compensated by downward BPA.

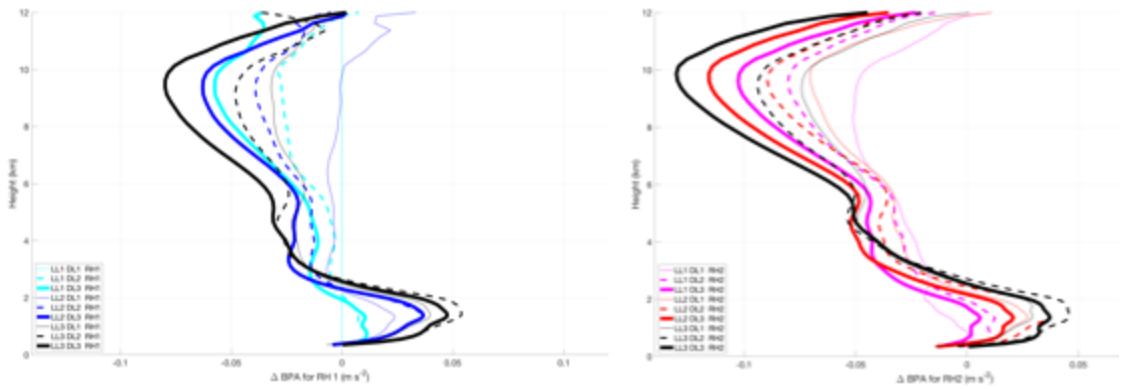

Figure 13. As in Figure 6, but for BPA horizontally averaged over updraft regions.

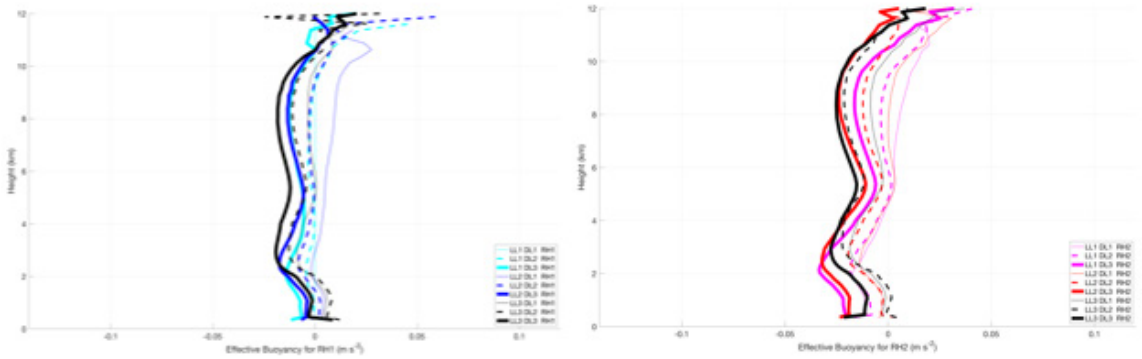

Figure 14. As in Figure 6, but for EBPA horizontally averaged over updraft regions

Recall that DPA encapsulates vertical accelerations that result from mechanical interactions between the environmental shear and the squall line structure. We must therefore examine the vertical distribution of DPA to address hypothesis two. For instance, the convergence and vorticity associated with the interaction between shear and the outflow edge often results in strong upward DPA in the lower atmosphere. Likewise, convergence and vorticity associated with the interaction between shear aloft and updraft cores can lead to upward accelerations. Figure 15 shows effects of shear on DPA. In general, both larger

low-level and deep-layer shear lead to stronger upward DPA. Shear influences on DPA are locally pronounced at low-levels, suggesting that shear interactions with the cold pool become stronger as both low-level and deep-layer shear are enhanced. Shear influences on DPA are also locally pronounced at upper-levels, suggesting that progressively stronger shear equates to shear interactions with updrafts that drive stronger upward accelerations.

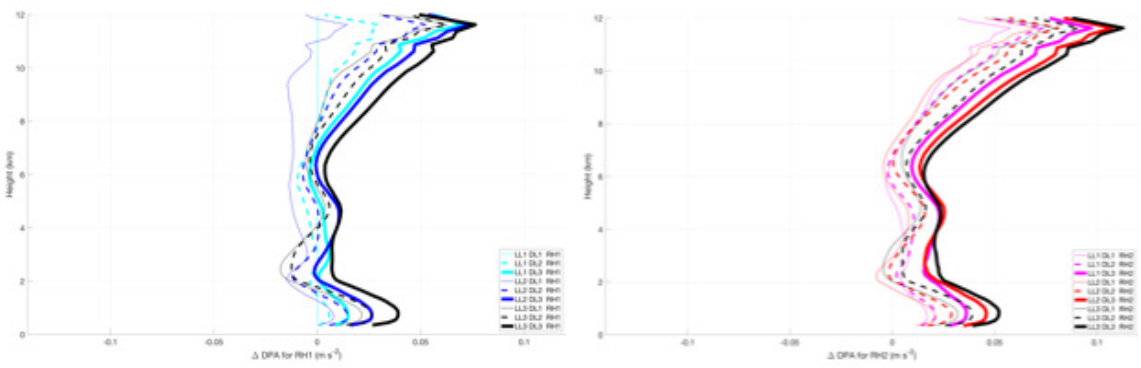

Figure 15. As in Figure 6, but for DPA horizontally averaged over updraft regions

Determinations about the relative importance of each acceleration term can be made by analyzing changes to the vertical accelerations. Figure 16 shows how shear effects the net differences in vertical accelerations. At lower levels of the atmosphere, increases to low-level shear overshadow increases to deep-layer shear. In the plots of buoyancy, EBPA, and DPA this relationship is not as apparent. Comparing the values of DPA (Figure 15) and EBPA (Figure 14) in lowest levels of the atmosphere it is clear that increases to DPA drive low level accelerations. While increasing shear makes squall lines more buoyant, those increases in buoyancy are largely canceled by increases in downward BPA. The primary way that shear intensifies squall lines is by making stronger dynamic accelerations in the lowest part of the atmosphere.

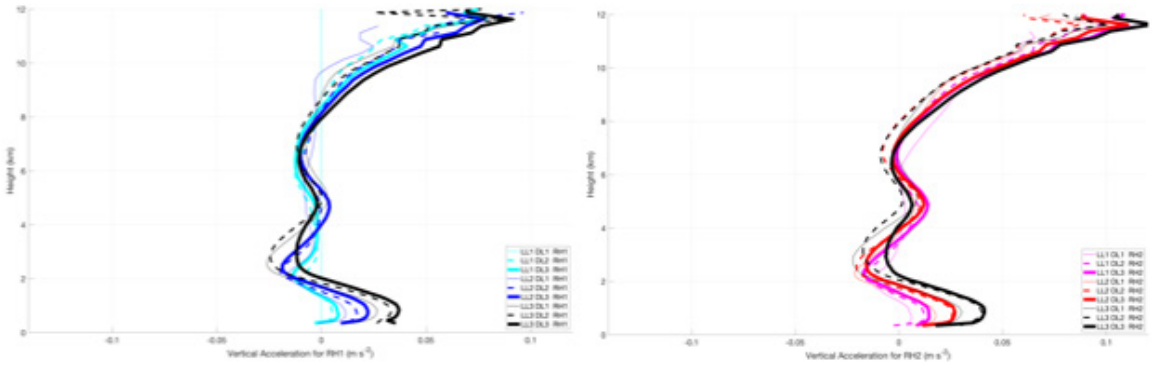

Figure 16. As in Figure 6, but for the sum of buoyancy and all pressure accelerations

As a final assessment of the practical impacts of the shear modulation of updraft strength on squall lines' sensible weather impacts, the differences in the maximum near-surface wind speeds, shown in Figure 17, were examined. Recall that larger near-surface winds speeds equate to a greater potential for damaging wind production. In general, increases in shear velocity cause increases in maximum surface wind speed. With lower humidity values there was less separation between the shear values. At higher humidity values, the model runs with the highest deep-layer shear values (LL3_DL3_RH2 - black line and LL2_DL3_RH2 - red line) caused a ~ 5 m s^{-1}, hour long, spike in surface wind speed. These intensification spikes and general trend of wind speed prove that squall line intensity increases with increasing shear values.

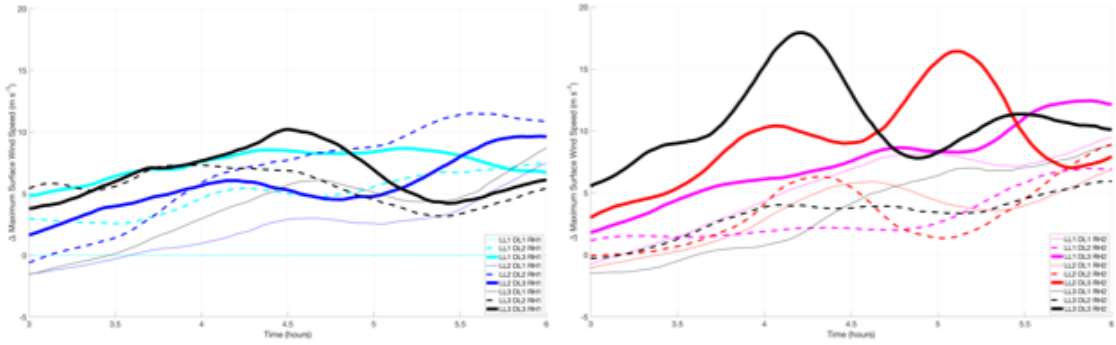

Figure 17. Average maximum surface wind speed

THIS PAGE INTENTIONALLY LEFT BLANK

V. SUMMARY, CONCLUSIONS, AND FUTURE WORK

This paper investigated how low-level and deep-layer shear effect the intensity of squall lines by looking at the links between shear, entrainment, and vertical accelerations. The links were analyzed using 3D computer model simulations, with initial conditions known to generate squall lines, and within which the low-level and deep-layer shear were varied. To examine the effects of shear on entrainment plots of buoyant updrafts, maximum tracer concentration, and vertical pressure accelerations were analyzed. To examine the effects of shear on squall line intensity, plots of vertical mass flux, vertical velocity, and maximum surface wind speed were analyzed. Based on the analysis of simulations, conclusions are as follows:

1. Increasing both low-level and deep-layer shear increase maximum updraft velocities in squall line updrafts.

2. Mid-level updraft buoyancy generally increases as shear increases, because larger shear equates to larger vertical mass flux and greater updraft area accordingly. The more expansive updraft area in the strongly sheared runs equated to updraft cores that were more shielded from entrainment-driven dilution.

3. The increases in updraft buoyancy with increasing shear, however, were largely canceled by commensurate increases in downward oriented buoyancy pressure accelerations. This suggests that hypothesis one is not a plausible explanation for why shear makes squall line updrafts more intense.

4. Shear generally increases upward dynamic pressure accelerations throughout updrafts, which resulted in much larger net accelerations at low-levels in strongly sheared runs than in weakly sheared runs. This supports hypothesis two.

Previous scientific work on shear looked at low-level and deep-layer separately with most of the research focusing on the effects of low-level shear. Coniglio et al. (2006) confirmed that deep-layer shear strengthens squall lines but did not detail the dynamics involved. Additionally, debates continue over whether low-level or deep-layer shear is more important to squall line intensity. This paper advanced these contentious areas by studying the effects of low-level and deep-layer shear, both separately and together. It details the dynamic changes caused by both. Lastly, it provides additional evidence for the importance of both low-level and deep-layer shear.

While a lot of data was covered in this paper it focused mostly on trends and averages but did not directly quantify the results. There are still many areas for future work. Is there a linear link between shear and entrainment? When does the updraft area become significantly large enough that it insulates the updraft core from entrainment? Or is there a tipping point where shear and updraft area cause a rapid decrease in entrainment. The simulations here were run at a 2 km horizontal grid spacing because of limited computational resources. While previous studies have shown that this resolution is sufficient to capture the macro scale features in squall lines (e.g. Done et al. 2004), the character of updrafts in squall lines changes considerably when the horizontal grid spacing is 250 m or finer (e.g. Lebo and Morrison 2015). How might model resolution affect our results?

LIST OF REFERENCES

American Meteorological Society, 2019: Mesoscale Convective System. Glossary of Meteorology. Accessed 12 February 2019, http://glossary.ametsoc.org/wiki/climatology.

Bryan, G.H., and R. Rotunno, 2014: The Optimal State for Gravity Currents in Shear. *J. Atmos. Sci.*, **71,** 448–468, https://doi.org/10.1175/JAS-D-13-0156.1.

Coniglio, M.C., D.J. Stensrud, and L.J. Wicker, 2006: Effects of Upper-Level Shear on the Structure and Maintenance of Strong Quasi-Linear Mesoscale Convective Systems. *J. Atmos. Sci.*, **63**, 1231–1252, https://doi.org/10.1175/JAS3681.1.

Coniglio, M.C., J.Y. Hwang, and D.J. Stensrud, 2010: Environmental Factors in the Upscale Growth and Longevity of MCSs Derived from Rapid Update Cycle Analyses. *Mon. Wea. Rev.*, **138**, 3514–3539, https://doi.org/10.1175/2010MWR3233.1.

Done, J., Davis, C. A., and Weisman, M. (2004), The next generation of NWP: explicit forecasts of convection using the weather research and forecasting (WRF) model. *Atmosph. Sci. Lett.,* **5**, 110-117. doi:10.1002/asl.72.

Erdman, Jonathan, 2018: How Missouri Duck Boat tragedy unfolded: Timeline of weather watches, warnings, reports. The Weather Channel. Accessed 20 June 2018, https://weather.com/storms/severe/news/2018-07-20-missouri-duck-boat-table-rock-lake-weather-timeline.

Gallus, W.A., N.A. Snook, and E.V. Johnson, 2008: Spring and Summer Severe Weather Reports over the Midwest as a Function of Convective Mode: A Preliminary Study. *Wea. Forecasting*, **23**, 101–113, https://doi.org/10.1175/2007WAF2006120.1.

Grant, L.D., T.P. Lane, and S.C. van den Heever, 2018: The role of cold pools in tropical oceanic convective systems. *J. Atmos Sci.*, **75**, 2615-2634.

Guastini, C.T., and L.F. Bosart, 2016: Analysis of a Progressive Derecho Climatology and Associated Formation Environments. *Mon. Wea. Rev.*, **144**, 1363–1382, https://doi.org/10.1175/MWR-D-15-0256.1

Hamilton, R. A., and J. W. Archbold, 1945: Meteorology of Nigeria and adjacent territory. *Quart. J. Roy. Metor. Soc.*, **71**, 231–262.

Holle, R.L., A.I. Watson, R.E. López, D.R. Macgorman, R. Ortiz, and W.D. Otto, 1994: The Life Cycle of Lightning and Severe Weather in a 3–4 June 1985 PRE-STORM Mesoscale Convective System. *Mon. Wea. Rev*., **122**, 1798–1808, https://doi.org/10.1175/1520-0493(1994)122<1798:TLCOLA>2.0.CO;2.

Houze, R.A., 1977: Structure and Dynamics of a Tropical Squall–Line System. *Mon. Wea. Rev.,* **105**, 1540–1567, https://doi.org/10.1175/1520-0493(1977)105<1540:SADOAT>2.0.CO;2.

Johns, R.H., 1993: Meteorological Conditions Associated with Bow Echo Development in Convective Storms. *Wea. Forecasting*, **8**, 294–299, https://doi.org/10.1175/1520-0434(1993)008<0294:MCAWBE>2.0.CO;2.

Johns, R.H., and C.A. Doswell, 1992: Severe Local Storms Forecasting. *Wea. Forecasting*, 7, 588–612, https://doi.org/10.1175/1520-0434(1992)007<0588:SLSF>2.0.CO;2.

Johns, R.H., and W.D. Hirt, 1987: Derechos: Widespread Convectively Induced Windstorms. *Wea. Forecasting*, **2**, 32–49, https://doi.org/10.1175/1520-0434(1987)002<0032:DWCIW>2.0.CO;2.

Lebo, Z.J., and H. Morrison, 2015: Effects of Horizontal and Vertical Grid Spacing on Mixing in Simulated Squall Lines and Implications for Convective Strength and Structure. *Mon. Wea. Rev.*, **143**, 4355–4375, https://doi.org/10.1175/MWR-D-15-0154.1

Makowski, J.A., D.R. MacGorman, M.I. Biggerstaff, and W.H. Beasley, 2013: Total Lightning Characteristics Relative to Radar and Satellite Observations of Oklahoma Mesoscale Convective Systems. *Mon. Wea. Rev*., **141**, 1593–1611, https://doi.org/10.1175/MWR-D-11-00268.1.

Markowski, P, and Y. Richardson, 2010: Mesoscale Convective Systems. *Mesoscale Meteorology in Midlatitudes*, John Wiley and Sons, Ltd, 245–269.

Markowski, P, and Y. Richardson, 2010: Organization of Isolated Convection. *Mesoscale Meteorology in Midlatitudes*, John Wiley and Sons, Ltd, 202–242.

Morrison, H., 2016: Impacts of Updraft Size and Dimensionality on the Perturbation Pressure and Vertical Velocity in Cumulus Convection. Part I: Simple, Generalized Analytic Solutions. *J. Atmos. Sci.*, **73**, 1441–1454, https://doi.org/10.1175/JAS-D-15-0040.1.

Morrison, H., 2016: Impacts of Updraft Size and Dimensionality on the Perturbation Pressure and Vertical Velocity in Cumulus Convection. Part II: Comparison of Theoretical and Numerical Solutions and Fully Dynamical Simulations. *J. Atmos. Sci*., **73**, 1455–1480, https://doi.org/10.1175/JAS-D-15-0041.1.

National Severe Storms Laboratory, 2019: Thunderstorm basics. Accessed 12 Feb 2019, https://www.nssl.noaa.gov/education/svrwx101/thunderstorms.

Parker, M.D., 2010: Relationship between System Slope and Updraft Intensity in Squall Lines. *Mon. Wea. Rev.*, 138, 3572–3578, https://doi.org/10.1175/2010MWR3441.1

Parker, M.D., and R.H. Johnson, 2000: Organizational Modes of Midlatitude Mesoscale Convective Systems. *Mon. Wea. Rev*., **128**, 3413–3436, https://doi.org/10.1175/1520-0493(2001)129<3413:OMOMMC>2.0.CO;2.

Peters, J.M., 2016: The Impact of Effective Buoyancy and Dynamic Pressure Forcing on Vertical Velocities within Two-Dimensional Updrafts. *J. Atmos. Sci*., **73**, 4531–4551, https://doi.org/10.1175/JAS-D-16-0016.1.

Peters, J.M., W. Hannah, and H. Morrison, 0: The influence of vertical wind shear on moist thermals. *J. Atmos. Sci*., In Press, https://doi.org/10.1175/JAS-D-18-0296.1.

J. M. Peters, Nowotarski, C. J., and Morrison, H., 2019. Submitted to the Journal of Atmospheric Science.

Rotunno, R., J. B. Klemp, and M. L. Weisman, 1988: A theory for strong, long-lived squall lines. J. *Atmos. Sci.*, **45**, 463–485, https://doi.org/10.1175/1520-0469(1988)045<0463:ATFSLL>2.0.CO;2.

Rutledge, S.A., and D.R. MacGorman, 1988: Cloud-to-Ground Lightning Activity in the 10–11 June 1985 Mesoscale Convective System Observed during the Oklahoma–Kansas PRE-STORM Project. *Mon. Wea. Rev*., **116**, 1393–1408, https://doi.org/10.1175/1520-0493(1988)116<1393:CTGLAI>2.0.CO;2.

Schumacher, R.S., and R.H. Johnson, 2005: Organization and Environmental Properties of Extreme-Rain-Producing Mesoscale Convective Systems. *Mon. Wea. Rev*., **133**, 961–976, https://doi.org/10.1175/MWR2899.1.

Stensrud, D.J., M.C. Coniglio, R.P. Davies-Jones, and J.S. Evans, 2005: Comments on "'A Theory for Strong Long-Lived Squall Lines' Revisited." *J. Atmos. Sci.,* **62**, 2989–2996, https://doi.org/10.1175/JAS3514.1

Weisman, M.L., and R. Rotunno, 2004: "A Theory for Strong Long-Lived Squall Lines" Revisited. *J. Atmos. Sci.*, **61**, 361–382, https://doi.org/10.1175/1520-0469(2004)061<0361:ATFSLS>2.0.CO;2.

Weisman, M.L., and R. Rotunno, 2005: Reply. *J. Atmos. Sci*., **62**, 2997–3002, https://doi.org/10.1175/JAS3515.1.

THIS PAGE INTENTIONALLY LEFT BLANK

INITIAL DISTRIBUTION LIST

1. Defense Technical Information Center
   Ft. Belvoir, Virginia

2. Dudley Knox Library
   Naval Postgraduate School
   Monterey, California